

# Estimating Peak Velocity Profiles from Doppler Echocardiography using Digital Image Processing

Amirtahà Taebi<sup>1,2,\*</sup>, Richard H. Sandler<sup>2,3</sup>, Bahram Kakavand<sup>4</sup>, Hansen A. Mansy<sup>2</sup>

<sup>1</sup>Department of Biomedical Engineering, University of California, Davis, CA 95616, USA

<sup>2</sup>Biomedical Acoustics Research Laboratory, University of Central Florida, Orlando, FL 32816, USA

<sup>3</sup>College of Medicine, University of Central Florida, Orlando, FL 32827, USA

<sup>4</sup>Department of Cardiovascular Services, Nemours Children's Hospital, Orlando, FL 32827, USA

ataebi@ucdavis.edu, hansen.mansy@ucf.edu, rhsandler@gmail.com, bahram.kakavand@nemours.org

**Abstract**—This study aims at developing a digital signal processing algorithm to extract positive and negative peak velocity profiles from Doppler echocardiographic images. These profiles are useful in estimating cardiac time intervals and establishing realistic boundary conditions for computational hemodynamic studies. The proposed image processing algorithm is based on two different thresholding methods. The histograms of image intensity function were used to help threshold values selection so that the algorithm yields velocity profiles properly represent Doppler shift envelopes. One of the thresholding methods tended to provide the lower-limit (i.e. underestimate) of the velocity profile, while the second tended to provide the upper-limit of the velocity profile (i.e., overestimate). The final peak velocity profiles were estimated from the combination of the estimates from both thresholding methods. The peak velocity profiles were then qualitatively compared with the results of the standard edge detection methods such as Canny and Prewitt approximations. The proposed automated approach might be helpful for objective estimation of peak velocities and cardiac time intervals.

**Keywords**—Doppler echocardiography; Doppler shift; peak velocity profile; thresholding; image processing; Canny approximation; Prewitt approximation.

## I. INTRODUCTION

Cardiovascular disease is one of the leading causes of death in the world [1]. Doppler echocardiography is a common method used to provide quantitative and qualitative diagnostic information about blood flow velocity and direction. In addition, the measured velocity profiles are used in clinical settings to determine cardiac time intervals which would provide useful information for various cardiovascular conditions [2]–[5]. These velocity profiles also have utility in research studies of cardiac physiology and hemodynamics. For example, profiles are useful in elucidating the relationship between physiological processes and cardiac signals such as seismocardiography [6], [7]. Profiles can also be used to develop realistic boundary conditions in computational fluid dynamics simulations of the heart and arteries, and can potentially lead to more accurate predictions of local and systemic hemodynamics [8]–[10]. Peak flow velocities in different cardiac phases, including systolic, early and late diastolic are also measured from these velocity profiles [11].

Image processing and edge detection techniques have been used in various medical research studies [12], [13] including Doppler ultrasound processing and extraction of velocity

profiles from these images [14]–[17]. In this paper, a new image processing algorithm is presented for the automatic extraction of peak velocity profile from Doppler echocardiographic images which is less computationally expensive compared to the available methods in literature. This paper is organized as follows. Section II provides information about the image acquisition methods and the proposed image processing algorithm. The results are reported and discussed in section III, followed by conclusions in section IV.

## II. METHODOLOGY

Doppler echocardiography data was recorded from the video monitor of a Doppler machine (Model: EPIQ 5, Philips, Netherlands) using a video recorder (Model: CA-998P, HDML Cloner Box Pro, ClonerAlliance, USA) at a frame rate of 30 frames per second. The echocardiography video frames were then read as 8-bit unsigned integer images using MATLAB (R2015b, The MathWorks, Inc., Natick, MA).

The images were considered as a scalar function  $f(X, Y)$ , where  $X \in x = [1, \dots, m]$  and  $Y \in y = [1, \dots, n]$ , and  $m$  and  $n$  are the number of pixels in the horizontal and vertical directions, respectively. Fig. 1 shows a sample Doppler echocardiography image (i.e., 1 frame of the recorded video) taken from the center of the mitral valve of a 55-year-old male with no history of heart disease. In this figure,  $m$  and  $n$  are 1920 and 1080, respectively. The Doppler baseline (i.e., zero velocity) is shown as a yellow solid line at  $Y_{base} = 790$ . Positive and negative shifts are displayed above and below this line, and indicate blood flow towards and away from the transducer, respectively. The subject electrocardiographic signal (green solid line) is also shown in Fig. 1.

An image processing algorithm was developed to extract peak velocity profiles from the echocardiography images. The algorithm was based on identification and thresholding of gray color pixels in the echocardiography images and it can be summarized in the following steps:

- i. The original echocardiographic image (such as the one shown in Fig. 1) is loaded.
- ii. A region of interest (ROI) is defined such that it only contains the Doppler shift ( $1 < x < m$ ,  $n_{up} < y < n_{lo}$ ), where  $n_{up}$  and  $n_{lo}$  are the upper and lower borders of the ROI, respectively. Pixels outside the ROI are then

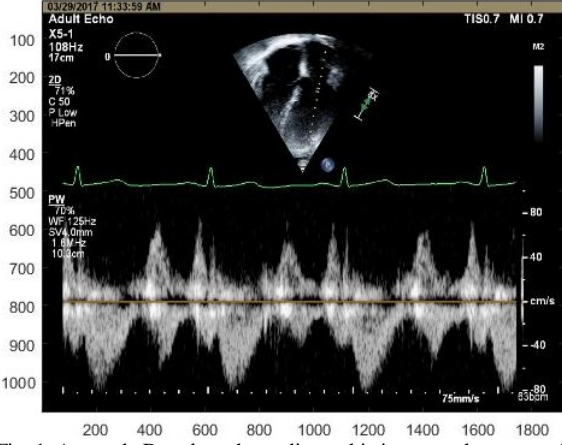


Fig. 1. A sample Doppler echocardiographic image at the center of the mitral valve taken from a 55-year-old male subject with no history of heart disease. The horizontal and vertical axes represent the number of pixels.

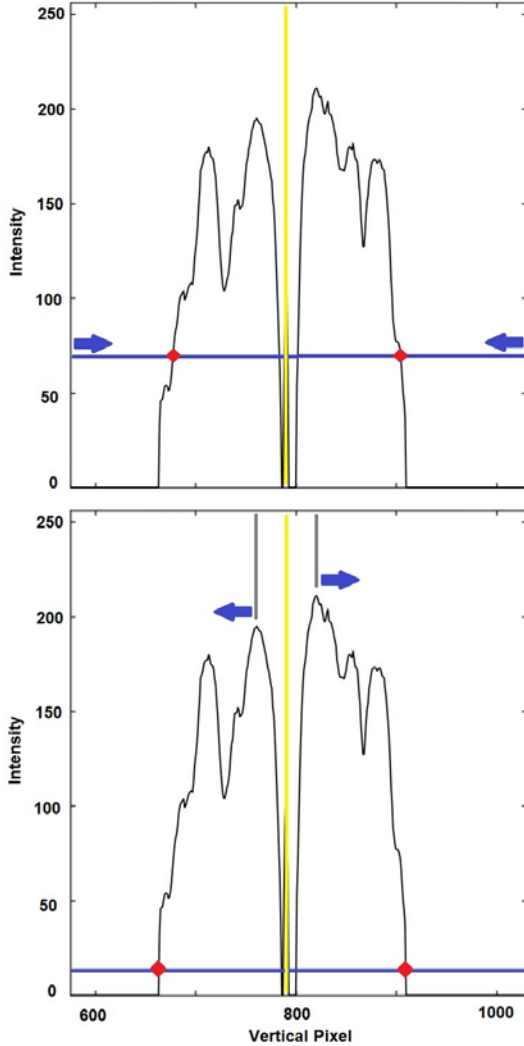


Fig. 2. Edge detection using (up) method 1, and (bottom) method 2. The averaged intensity is shown for ( $X = 600, n_{up} < y < n_{lo}$ ). Yellow line: baseline, blue line: threshold, gray line: maximum intensity before and after the baseline, blue arrows: sweeping direction, red dots: upper and lower detected edges.

removed. For instance, all pixels above  $n_{up} = 575$  and below  $n_{lo} = 1030$  in Fig. 1 are removed.

- iii. The gray scale intensity of pixels is calculated. For this purpose, the average RGB intensity,  $\mu$ , at pixel ( $X \in x, Y \in y$ ) is calculated as:

$$\mu = (R + G + B)/3, \quad (1)$$

where  $R, G$ , and  $B$  are the intensities of red, green, and blue components at  $(X, Y)$ , respectively.

- iv. The RGB image is then smoothed by a moving average process. The smoothed image intensity,  $I_{smooth}$ , at  $(X, Y)$  is calculated as the mean intensity of a  $(2p + 1) \times (2q + 1)$  rectangle centered at  $(X, Y)$ :

$$I_{smooth}(X, Y) = \frac{\sum_{j=Y-q}^{Y+q} \sum_{i=X-p}^{X+p} I(i, j)}{(2p + 1)(2q + 1)}, \quad (2)$$

where  $I$  is the image intensity (i.e., RGB values) before smoothing. In this study, the results are shown for  $p = q = 3$ .

- v. The maximum  $\mu$  intensity at each vertical line (i.e., at each  $X \in x$ ) is found within the ROI. This value is called  $\mu_{max,X}$ .
- vi. Gray pixel edges are detected using two different thresholding methods. In the first method (Fig. 2, up panel), edge search starts at upper and lower borders of the ROI and moves towards the baseline. The upper and lower edges of the Doppler shift at each  $X$  are chosen as the smallest and largest  $Y \in (n_{up} < y < n_{lo})$  such that  $\mu(X, Y) > \theta_1 \mu_{max,X}$ , where  $\theta_1$  is the threshold value (solid blue line in Fig. 2). This method is designed to provide a lower-limit of the velocity magnitude.

In the second method (Fig. 2, bottom panel), edge search starts from the pixels where maximum intensity occurs before and after the baseline (vertical gray lines in Fig. 2, bottom panel), and it moves towards the ROI borders. The upper edge at each  $X$  is found as the smallest  $Y \in (n_{up} < y < Y_{base})$  such that  $\mu(X, Y) < \theta_2 \mu_{max,X}$ . The lower edge is calculated as the largest  $Y \in (Y_{base} < y < n_{lo})$  such that  $\mu(X, Y) < \theta_2 \mu_{max,X}$ . This method is designed to provide an upper-limit of the velocity magnitude.

The intensity histograms of the ROI consisted of two main peaks around gray intensities of 0 and 175. The first peak corresponds to the black background. The second peak falls in the gray color RGB range of the Doppler shift. The threshold values for both methods,  $\theta_1$  and  $\theta_2$ , were chosen to be between the two peaks such that their resulting velocity profiles agree with the expert opinion of the study clinicians.

- vii. The positive peak velocity profile for each thresholding method is constructed by connecting the upper edges detected in Step vi above. The negative

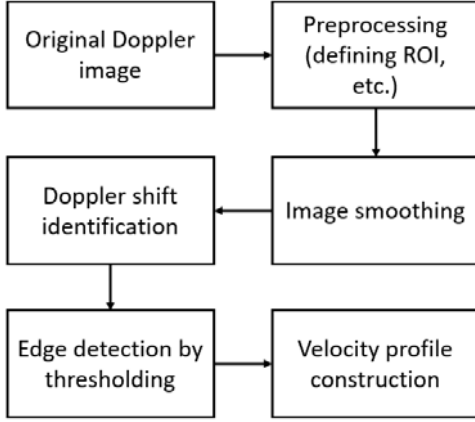


Fig. 3. Proposed image processing algorithm for peak velocity profile extraction from Doppler echocardiographic images.

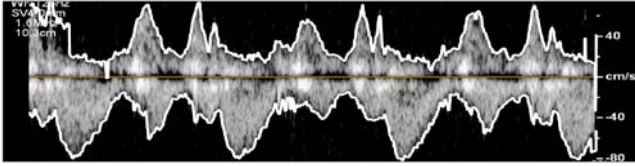


Fig. 4. Positive and negative peak velocity profiles extracted from the proposed algorithm.

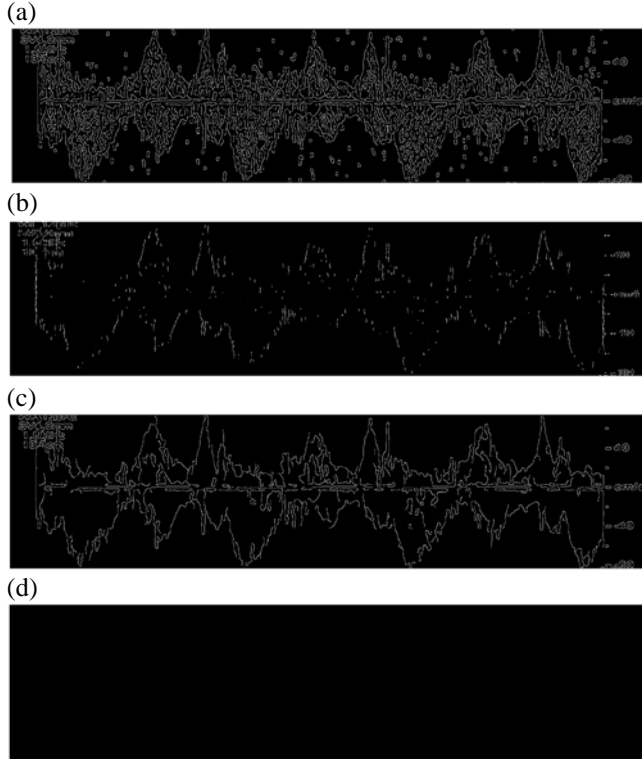


Fig. 5. Edge detection results from standard edge detection methods. (a) Canny approximation with a threshold of 0.05, (b) Prewitt method with a threshold of 0.05, (c) Canny approximation with a threshold of 0.3, and (d) Prewitt method with a threshold of 0.3.

peak velocity profile for each thresholding method is similarly constructed by connecting the lower edges.

- viii. The two proposed thresholding methods in Step vi estimate the peak velocity differently and necessitate different threshold values. The first method starts searching for the peak velocity at the ROI borders (see the blue arrows in Fig. 2, up panel) and uses relatively higher threshold to avoid artifacts at the borders. This method estimates a lower-limit (underestimate) for the peak velocity magnitude. In contradistinction, the second method starts searching for the peak velocity from baseline (see the blue arrows in Fig. 2, bottom panel) and uses a lower threshold, which would estimate an upper-limit (overestimate) of the peak velocity profile. The estimated velocity profiles from both methods are averaged to construct the velocity profiles. The averaged profiles,  $P_{avg}$ , are calculated as:

$$P_{avg,up} = P_{1,up} + P_{2,up}, \quad (3)$$

$$P_{avg,lo} = P_{1,lo} + P_{2,lo}, \quad (4)$$

where  $P_{1,up}$  and  $P_{1,lo}$  are the upper and lower limits of the peak velocity profile from thresholding method 1, respectively.  $P_{2,up}$  and  $P_{2,lo}$  are the upper and lower limits of the peak velocity profile from thresholding method 2, respectively. The proposed algorithm is summarized in Fig. 3.

The edges of the Doppler shift (i.e., peak velocity profiles) are also detected using two standard edge detection methods including Canny and Prewitt. In both methods, the gradient of the image intensity function is calculated (e.g., using the derivative of a Gaussian filter in Canny method). The edges are then found by looking for local maxima of the gradient [18].

### III. RESULTS AND DISCUSSIONS

Fig. 4 shows the peak velocity profiles extracted from the Doppler image using the proposed method. The proposed algorithm incorrectly estimated the positive peak velocity profile at the upper left edge of the ROI. In this portion of ROI ( $1 < x < 200$ ,  $500 < y < 700$  of the original image), there was some white text. Since the first thresholding method scanned the pixels at each vertical line starting from the borders of the ROI, this error resulted. The proposed method, however, estimated the peak velocity profiles correctly in the other ROI regions. The standard edge detection methods used in this study (i.e., Canny and Prewitt) were tested for different thresholding values in the range of 0.02 – 0.5. Fig. 5 shows the edge detection results obtained from these methods for 2 sample thresholding values of 0.05 and 0.3. First, Canny approximation with a threshold of 0.05 was used to detect the Doppler shift edges in vertical direction (Fig. 5.a). Although the method detected the Doppler shift edges, it detected too many other edges either inside or outside of Doppler shift. A higher threshold can be used to reduce these extra unwanted edges. This is shown for a threshold value of 0.3 (Fig. 5.c). Here, the number of artifacts drastically decreased. However, there are still some artifacts

around the baseline and Doppler shift borders. Fig. 5.b and 5.d show the edge detection results for Prewitt approximation with threshold values of 0.05 and 0.3, respectively. Results show that Prewitt approximation was not as efficient as Canny method in estimating the Doppler shift edges, and, in general, needed smaller thresholds. For example, this method did not detect any edges for the threshold value of 0.3 as shown in Fig. 5.d. This is in agreement with the fact that Prewitt method is more sensitive to noise compared to Canny method [18]. The proposed method introduced fewer extra edges and artifacts. It was also simpler and less computationally expensive than both standard edge detection methods since it was only based on two thresholding operations.

#### IV. CONCLUSIONS

An image processing algorithm based on thresholding was proposed to extract peak velocity profiles from Doppler echocardiography images in a simple and straightforward manner. Two different thresholding methods were employed to estimate the upper and lower limits of the peak velocity profiles. Doppler images were smoothed using moving average process to improve the quality of extracted velocity profiles. The upper and lower limits of the velocity profiles were averaged to calculate the peak velocity profiles. The proposed algorithm was more efficient and less computationally expensive than available edge detection methods including Prewitt and Canny approximations. These velocity profiles can be used in clinical and research studies including cardiac time intervals estimations and computational cardiovascular hemodynamics. Future work would quantitatively compare the estimates obtained in the current study with more standard edge detection methods along with validating these profiles using more accurate velocity profiles from invasive catheterization.

#### ACKNOWLEDGMENT

This study was supported by NIH R44HL099053. Authors would like to kindly appreciate the technical support of staff of the Department of Cardiology at Nemours Children’s Hospital, Orlando, FL.

Hansen A Mansy and Richard H Sandler are part owners of Biomedical Acoustics Research Company, which is the primary recipient of the above grant, as such they may benefit financially as a result of the outcomes of the research work reported in this publication.

#### REFERENCES

[1] “WHO, Cardiovascular diseases (CVDs),” *Fact sheets*. 2017.  
 [2] S. R. Ommen, R. a. Nishimura, C. P. Appleton, F. a. Miller, J. K. Oh, M. M. Redfield, and a. J. Tajik, “Clinical utility of Doppler echocardiography and tissue Doppler imaging in the estimation of left ventricular filling pressures: a comparative simultaneous Doppler....” *Circulation*, vol. 102, no. 15, pp. 1788–1794, 2000.  
 [3] T. Hozumi, T. Akasaka, K. Yoshida, and J. Yoshikawa, “Noninvasive estimation of coronary flow reserve by transthoracic Doppler

echocardiography with a high-frequency transducer,” *J. Cardiol.*, vol. 37 Suppl 1, pp. 43–50, 2001.  
 [4] T. Hozumi, K. Yoshida, T. Akasaka, Y. Asami, Y. Ogata, T. Takagi, S. Kaji, T. Kawamoto, Y. Ueda, and S. Morioka, “Noninvasive assessment of coronary flow velocity and coronary flow velocity reserve in the left anterior descending coronary artery by Doppler echocardiography: comparison with invasive technique,” *J. Am. Coll. Cardiol.*, vol. 32, no. 5, pp. 1251–1259, 1998.  
 [5] C. Y. Choong, V. M. Abascal, J. D. Thomas, J. Luis Guerrero, S. McGlew, and A. E. Weyman, “Combined influence of ventricular loading and relaxation on the transmitral flow velocity profile in dogs measured by Doppler echocardiography,” *Circulation*, vol. 78, no. 3 I, pp. 672–683, 1988.  
 [6] A. Taebi, R. H. Sandler, B. Kakavand, and H. A. Mansy, “Seismocardiographic Signal Timing with Myocardial Strain,” in *Signal Processing in Medicine and Biology Symposium (SPMB), 2017 IEEE*, 2017, pp. 1–2.  
 [7] A. Taebi, “Characterization, Classification, and Genesis of Seismocardiographic Signals,” University of Central Florida, 2018.  
 [8] F. Khalili, P. P. T. Gamage, and H. A. Mansy, “Prediction of Turbulent Shear Stresses through Dysfunctional Bileaflet Mechanical Heart Valves using Computational Fluid Dynamics,” in *3rd Thermal and Fluids Engineering Conference (TFEC)*, 2018, pp. 1–9.  
 [9] A. Sharifi, A. Salari, A. Taebi, H. Niazmand, and M. J. Niazmand, “Flow patterns and wall shear stress distribution in human vertebrobasilar system: A computational study to investigate smoking effects on atherosclerotic stenosis at different ages,” in *ASME International Mechanical Engineering Congress and Exposition, Proceedings (IMECE)*, 2017, vol. 3.  
 [10] F. Khalili, “Fluid Dynamics Modeling and Sound Analysis of a Bileaflet Mechanical Heart Valve,” University of Central Florida, 2018.  
 [11] H. F. Kuecherer, I. A. Muhiudeen, F. M. Kusumoto, E. Lee, L. E. Moulinier, M. K. Cahalan, and N. B. Schiller, “Estimation of mean left atrial pressure from transesophageal pulsed Doppler echocardiography of pulmonary venous flow,” *Circulation*, vol. 82, no. 4, pp. 1127–1139, 1990.  
 [12] A. Laine and Xuli Zong, “Border identification of echocardiograms via multiscale edge detection and shape modeling,” in *Proceedings of 3rd IEEE International Conference on Image Processing*, vol. 3, pp. 287–290.  
 [13] B. F. Vandenberg, L. S. Rath, P. Stuhlmuller, H. E. Melton, and D. J. Skorton, “Estimation of left ventricular cavity area with an on-line, semiautomated echocardiographic edge detection system,” *Circulation*, vol. 86, no. 1, pp. 159–166, 1992.  
 [14] A. Kathalia, Y. Karabiyik, S. H. Eik-Nes, E. Tegnander, I. K. Ekroll, G. Kiss, and H. Torp, “Adaptive Spectral Envelope Estimation for Doppler Ultrasound,” *IEEE Trans. Ultrason. Ferroelectr. Freq. Control*, 2016.  
 [15] Z. Ojaghi-Haghighi, H. Moladoust, M. Shojaeifard, M. Asadinezhad, and V. Nikseresht, “Comparison between methods used to extract maximum and minimum myocardial velocities by spectral pulsed-TDI,” *Iran. Cardiovasc. Res. J.*, vol. 5, no. 2, pp. 50–55, 2011.  
 [16] M. Zolgharni, N. M. Dhutia, G. D. Cole, K. Willson, and D. P. Francis, “Feasibility of using a reliable automated Doppler flow velocity measurements for research and clinical practices,” in *Progress in Biomedical Optics and Imaging - Proceedings of SPIE*, 2014.  
 [17] H. Greenspan, O. Shechner, M. Scheinowitz, and M. S. Feinberg, “Doppler echocardiography flow-velocity image analysis for patients with atrial fibrillation,” *Ultrasound Med. Biol.*, vol. 31, no. 8, pp. 1031–1040, 2005.  
 [18] R. Maini and H. Aggarwal, “Study and comparison of various image edge detection techniques,” *Int. J. Image Process.*, vol. 147002, no. 3, pp. 1–12, 2009.